ACS NANO

www.acsnano.org

ARTICLE

Ultra-Fast, Chemical-Free, Mass Production of High Quality Exfoliated Graphene

Aminul Islam,[#] Biswajyoti Mukherjee,[#] Krishna Kant Pandey, and Anup Kumar Keshri*

Cite This: *ACS Nano* 2021, 15, 1775−1784

Read Online

ACCESS | Metrics & More | Article Recommendations | Supporting Information

ABSTRACT: As graphene penetrates into industries, it is essential to mass produce high quality graphene sheets. New discoveries face formidable challenges in the marketplace due to the lack of proficient protocols to produce graphene on a commercial scale while maintaining its quality. Here, we present a conspicuous protocol for ultrafast exfoliation of graphite into high quality graphene on the sub-kilogram scale without the use of any intercalants, chemicals, or solvent. We show that graphite can be exfoliated using a plasma spray technique with high single-layer selectivity (~85%) at a very high production rate (48 g/h). This is possible because of the inherent characteristics of the protocol which provides sudden thermal shock followed by two-stage shear. The exfoliated graphene shows almost no basal defect (I_d/I_g: 0) and possesses high quality (C/O ratio: 21.2, sp^2 %: ~95%), an indication of negligible structural deterioration. The results were reproducible indicating the adeptness of the protocol. We provided several proofs-of-concept of plasma spray exfoliated graphene to demonstrate its utility in applications such as mechanical reinforcements; frictionless, transparent conductive coatings; and energy storage devices.

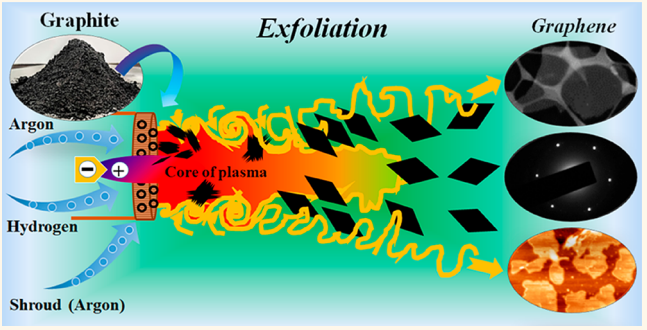

KEYWORDS: *exfoliation, graphene, 2D materials, chemical-free synthesis, mass production, defect-free, high quality*

As new protocols for graphene production emerge every day, the simultaneous fulfillment of four essential factors, *i.e.*, (1) high quality, (2) narrow layer distribution, (3) fast and reproducible technique, and (4) high throughput, has been far from satisfactory.[1−5] Graphene researchers face an uphill task of producing quality graphene on a large scale, key to bridging the gap between laboratory protocols and commercial applications. Nevertheless, considerable achievements have been made so far in the graphene realm, taking note of its future aspect. The bottom-up approach, chemical vapor deposition (CVD) or epitaxial growth, offers a large area (up to 7.5 m^2) of high quality graphene, crucial for advanced electronics.[6−10] Although recent contributions have tremendously reduced its cost of production, this still remains expensive due to multistep processes and lacks bulk production protocols, further limiting its niche of application.[2,5,9]

Thanks to cheap and abundant graphite sources, graphite can be exfoliated to graphene (top-down) on a large scale. The oxidation of graphite using strong acids or oxidants to form graphite oxide (GO) has proven to be a scalable precursor for reduced graphene oxide (rGO) with exfoliation yield close to 100%.[10−12] However, reduced graphene oxide contains high defects ($I_D/I_G \geq 1$) and low carbon content (60−80%) and possesses unimpressive carbon−oxygen ratio (C/O ≈ 10).[10,13,14] Despite efforts to minimize their defect concentration and subsequently increase carbon content, rGO is still considered a nonfeasible alternative to graphene. Electrochemical exfoliation, on the other hand, is a scalable approach to produce few-layer graphene (1−5 layers) with high yield (85%) with potential scale-up opportunities.[15−18] This technique, however, produces graphene with C/O ratio of 5−17 suggesting a trade-off between quantity and quality.[14,18] Mechanical exfoliation of graphite using a simple Scotch tape has provided the highest quality graphene in the past.[19] However, the fraction of single-layer graphene is negligible, and microscopic analysis is needed to separate them from graphite flakes, making it feasible only for laboratory tests. In this regard, shear exfoliation using liquid (liquid phase exfoliation) or ball milling has established itself as an inexpensive and versatile technique to exfoliate untreated graphite to graphene.[20−23] Although these protocols produce graphene with reduced defects ($I_D/I_G \approx 0.25$ or less) and high

Received: November 11, 2020
Accepted: January 13, 2021
Published: January 15, 2021

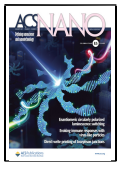

https://dx.doi.org/10.1021/acsnano.0c09451
ACS Nano 2021, 15, 1775−1784

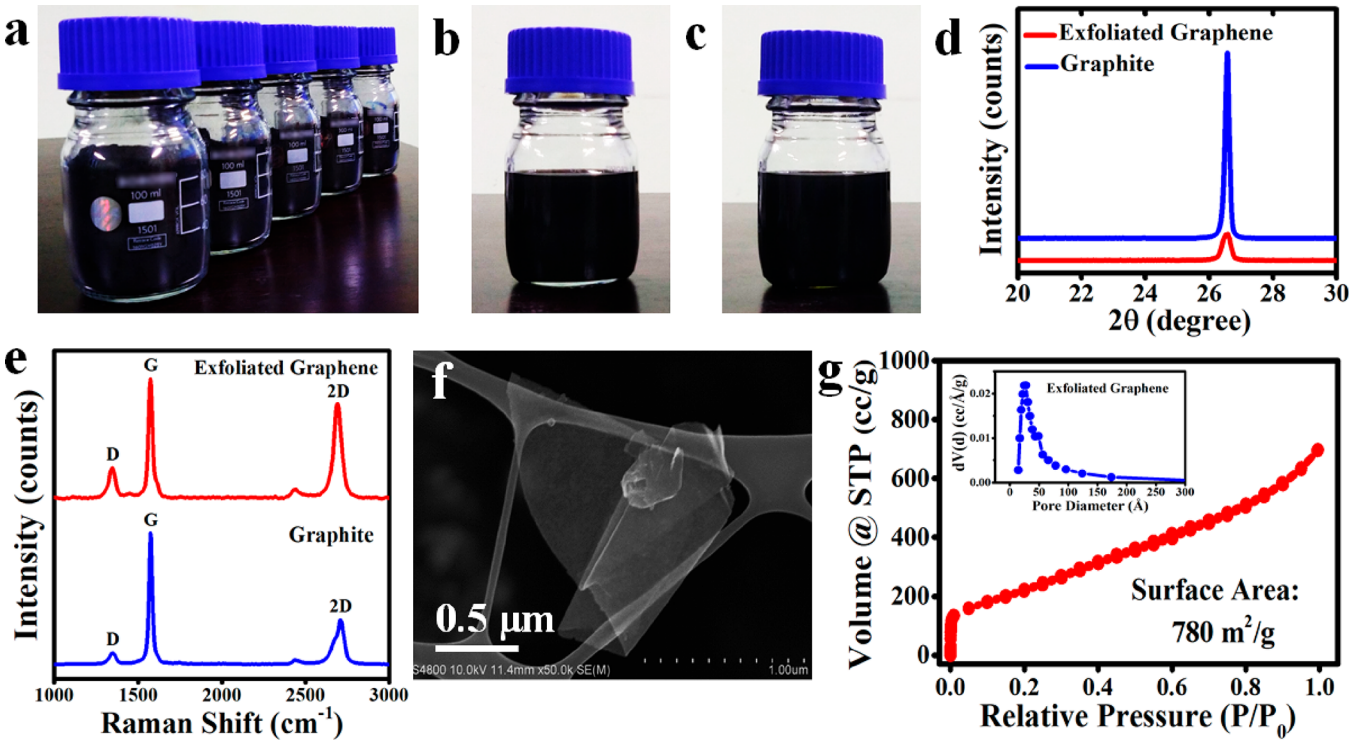

Figure 1. (a) Digital image of plasma spray exfoliated graphene. Each bottle contains 4 g of exfoliated graphene. (b) Dispersion of exfoliated graphene in organic solvents *N*-methylpyrrolidone (NMP) and (c) dimethylformamide (DMF) (concentration: 5 mg/mL). (d,e) X-ray diffraction (XRD) and Raman spectra of exfoliated graphene and graphite after plasma spraying. (f) Scanning electron microscopy (SEM) of exfoliated graphene drop-cast over a holey carbon grid. (Concentration: ~1 μg/mL in ethanol). (g) Nitrogen adsorption/desorption isotherm of exfoliated graphene; pore size distribution (inset).

C/O ratio (>20) compared to rGO and electrochemical exfoliated graphene, the long-term agitation results in unavoidable structural defects, which should be, in practice, free from defects.[24] Additionally, regardless of the high exfoliation efficiency (>90%), the statistical nature of exfoliation yields very low amount of single layer graphene (up to 5%).[20,21,23] Hence, realistically, even after 15 years of progress in graphene technology, a well-suited exfoliation method fulfilling all four requirements simultaneously is still missing.

Alternatively, graphene precursors exposed to high temperature (up to 4000 K) for milliseconds produces highly crystalline graphene with low defect concentration.[25] In the past, synthesis of graphene has been explored at high temperature either by (1) thermal shock of intercalated or expanded graphite[26] or by (2) gas-phase pyrolysis of alcohols.[27] Although the former offers a high production rate, the graphene contains high topological defects due to the rapid decomposition of functional groups. On the other hand, gas-phase synthesis, although promising, produces multilayer graphene with a high amount of amorphous carbon at a very low rate (~0.12 g/h).[27] A thorough review of past literature reveals that, although graphene synthesis at high temperature started back during 2003, the process could not establish itself due to stand-offs in all five factors. An overview of high-temperature-assisted graphene synthesis, a timeline of breakthroughs, and its limitations has been discussed thoroughly in the Supporting Information S1.

Herein, we demonstrate an ultrafast and scalable strategy to directly exfoliate graphite into high quality graphene with high selectivity toward single layer without the use of any intercalants, chemicals, or solvent. Exfoliation of graphite was accomplished using a DC plasma spray setup integrated with a custom-designed inert atmosphere shroud. The DC plasma spray system, inert atmosphere shroud, and in-flight particle diagnostic sensor are detailed in Supporting Information S2a,b. It is anticipated that all inherent features of this technique, *i.e.*, high quenching rate (~10^6 K/s), extremely low particle residence time (in μs), and dense eddies in turbulent region, could help in exfoliation of graphite into graphene. We achieved graphene with high single-layer selectivity (~85%), basal defect free (I_D/I_G = 0), and high purity (C/O ratio: 21.2; sp^2 % = 95%) with very high production rate of 48 g/h on the laboratory scale. Furthermore, the exfoliated graphene performs well in applications that require high quality graphene in large quantities. Our single-layer graphene showed high Young's modulus (850 GPa) and fine electrical conductivity under different bias voltage. The sheet resistance of the exfoliated graphene film was as low as 30 Ω/sq. In addition, the exfoliated graphene also demonstrated high specific capacitance value (375 F/g) and very low friction coefficient (COF = 0.03). In this study, we transformed a traditionally reserved technology for fabricating protective coatings into a protocol for ultrafast exfoliation of graphite to high quality graphene, which we believe could be a game-changer in this field.

RESULTS AND DISCUSSION

The graphite (detailed in Supporting Information S3) was directly introduced into the plasma plume without any pretreatment. We conducted multiple numbers of experiments with varying parameters (plasma power and primary gas flow

https://dx.doi.org/10.1021/acsnano.0c09451
ACS Nano 2021, 15, 1775−1784

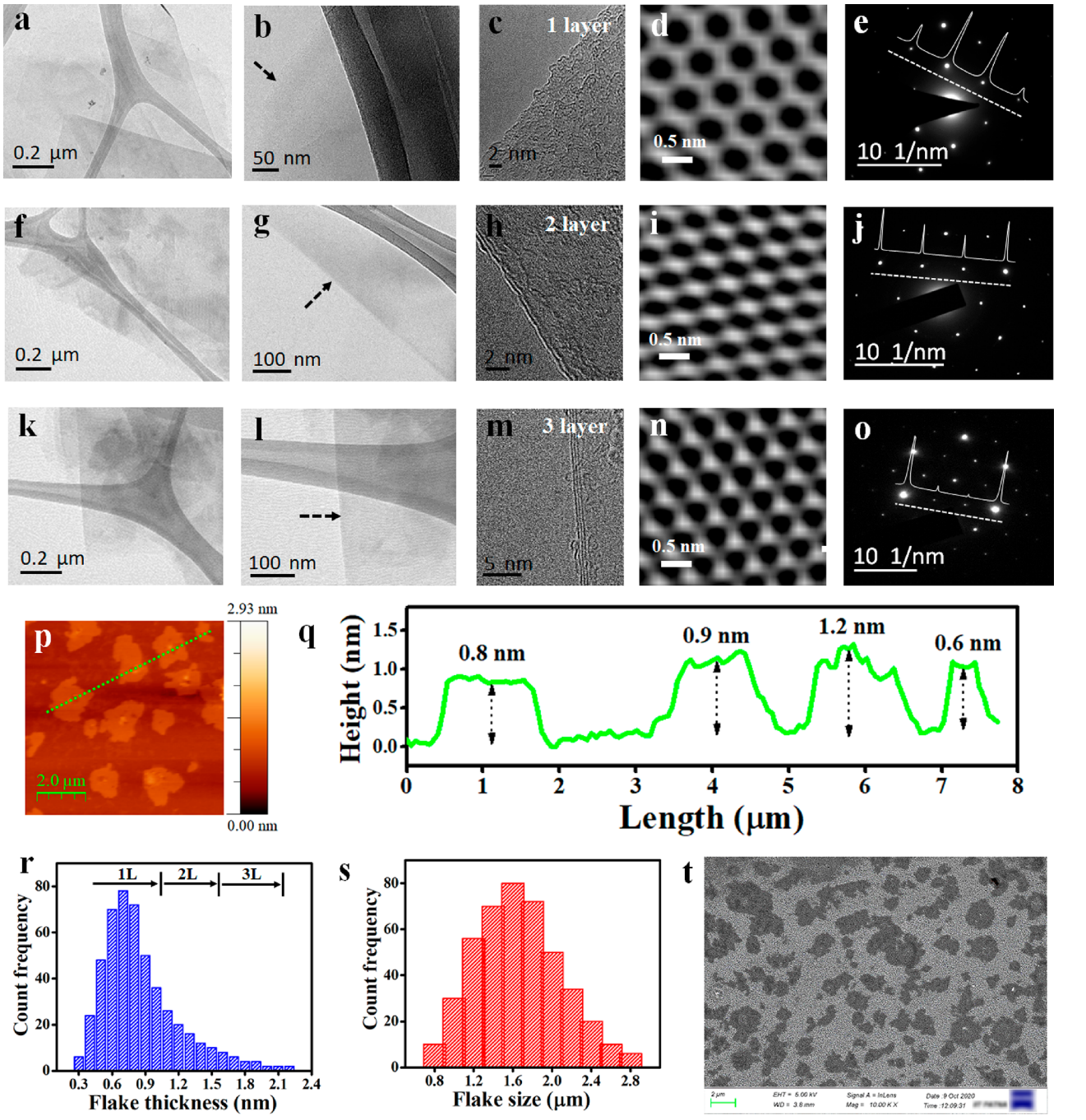

Figure 2. (a,b) Transmission electron microscopy (TEM) image of single-layer graphene. (c) High magnification image from edge of the single-layer graphene. (d) Butterworth filtered image of section of part c. (e) Selected area electron diffraction (SAED) pattern of the single-layer graphene. (f,g) TEM of a bilayer graphene. (h) Edges of the bilayer graphene show two graphene layers. (i) Filtered image of part h. (j) SAED pattern. (k,l) TEM of trilayer graphene. (m) Edges of the trilayer graphene. (n) Filtered image of part m. (o) SAED pattern. (p) Atomic force microscope of graphene. (q) Height profile along the dotted green line in part p. (r) Thickness and (s) length histogram of 400 selected arbitrary graphene flakes obtained using AFM. (t) Low magnification SEM image of the exfoliated graphene (drop-cast graphene over Si wafer).

rate) to get an idea about the parameter dependency on the exfoliation efficiency. The strategy behind choosing the process parameters has been discussed in Supporting Information S4. The plasma exposed graphite was collected and introduced to mild centrifugation (1000 rpm; 1 h) in deionized water to remove unexfoliated large agglomerates. After initial inspection using X-ray diffraction and Raman spectroscopy, we narrowed down to one parameter (plasma power (P): 40 kW, gas flow rate (G): 120 SCFH) which we presume is the best of the lot for exfoliated graphite (details about achieving the best parameter is included in Supporting Information S5−S8).

Figure 1a shows the digital image of the exfoliated graphene. A total of 20 g of exfoliated graphene was obtained after ∼25 min of plasma spraying, indicating scale-up potential. The exfoliated graphene remained dispersed in organic solvents (NMP and DMF) for 48 h without any surfactant stabilization (Figure 1b,c).The exfoliated graphene displays reduced X-ray diffraction (002) peak intensity at 2θ = 26.5°(Figure 1d)

https://dx.doi.org/10.1021/acsnano.0c09451
ACS Nano 2021, 15, 1775−1784

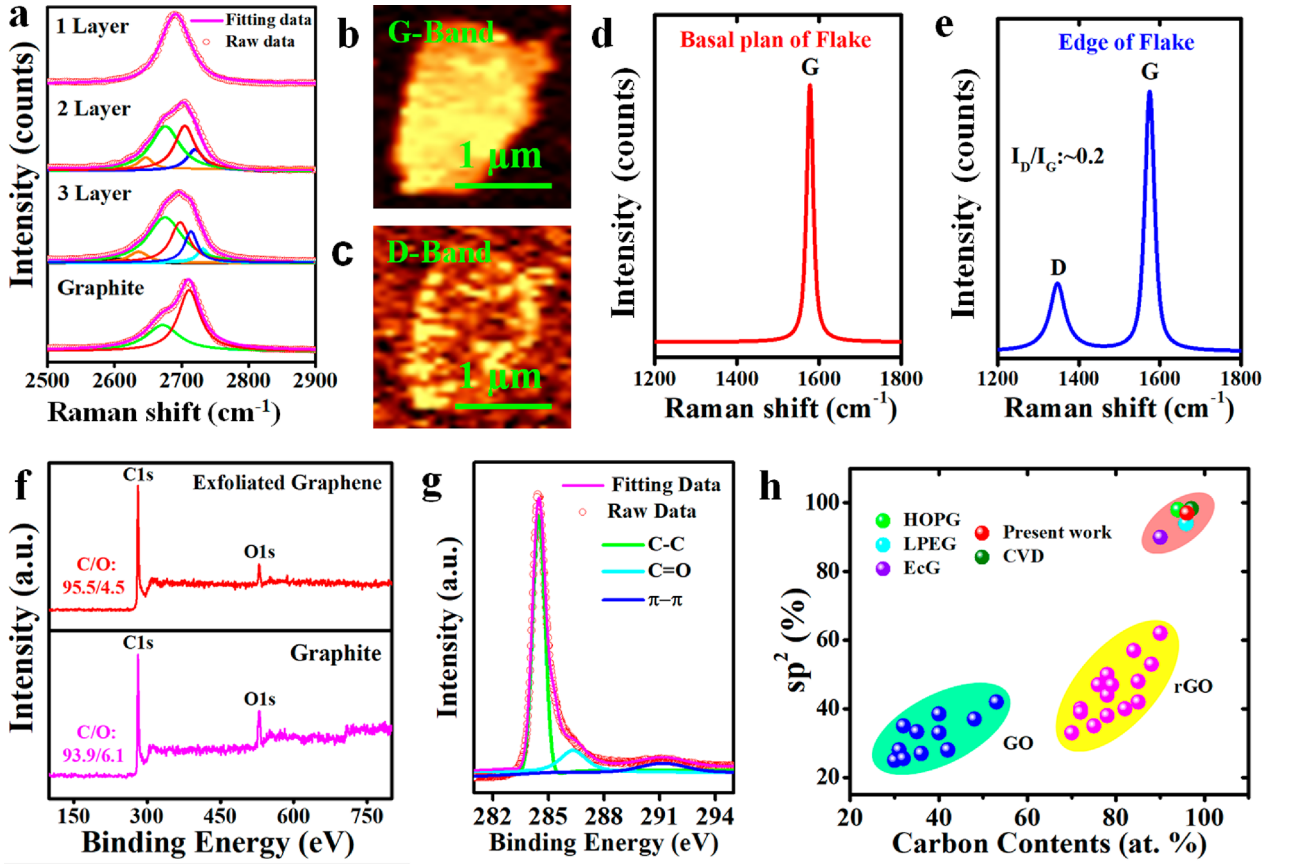

Figure 3. (a) Raman spectra, 2D band structure for single-layer, bilayer, trilayer graphene, and graphite. Raman map of a graphene flake generated from the intensity of (b) G and (c) D bands. Raman spectra collected from (d) mid and (e) edge of the flake using an *in situ* AFM–Raman. (f) X-ray photoelectron spectroscopy (XPS) survey of graphene. For comparison, XPS survey of graphite has also been included. Since XPS is surface sensitive, the samples were cleaned in RF plasma to avoid deposition of adventitious carbon. (g) Core-level carbon 1s XPS spectra of graphene. (h) Comparison of sp^2 and C content for GO, rGO, electrochemically exfoliated graphene (EcG), liquid-phase exfoliated graphene (LPEG), chemical vapor grown graphene (CVD), and graphite (including HOPG) with our exfoliated graphene. The values for GO, rGO, EcG, LPEG, and CVD are gathered from the literature.

suggesting high efficacy of graphite exfoliation.[28] Raman spectroscopy analysis (Figure 1e) shows a symmetric 2D band for the exfoliated graphene and confirms few-layer graphene which is clearly distinguishable from the graphite.[29] Shown in Figure 1f is the scanning electron microscopy (SEM) image of the exfoliated graphene. In comparison to the starting graphite (Supporting Information S3d,e), the exfoliated graphene flakes (more images in Supporting Information S9) are visually transparent indicating successful exfoliation of graphite to graphene. We also note that the lateral dimensions of these flakes are relatively large (1–3 μm), similar to the flakes obtained from LPE or milling using graphite of similar dimensions.[20,22] The size of graphene flakes was also verified by dynamic light scattering (Supporting Information S10). We also found a substantial increase in the surface area of our exfoliated graphite (780 m^2/g) (Figure 1g), comparable to the literature values (600–900 m^2/g) of few-layer graphene.[30] The pore size is ~5 nm for the exfoliated graphene (inset in Figure 1g).

We further analyzed individual graphene flakes using high resolution transmission electron microscope (HR-TEM). Figure 2a,f,k shows low-magnification basal images of individual graphene sheets, while Figure 2b,g,l is their corresponding magnified images. The edges of the flakes provide visual identification of layer numbers of the exfoliated graphene. A bright edge without a noticeable dark line as shown in Figure 2c is the characteristics of single layer graphene.[28] Alternatively, 2 and 3 dark fringes (Figure 2h,m) provide evidence of bilayer and trilayer graphene. Atomic resolution inverse Fourier images shows a perfect hexagonal pattern for the single layer graphene (Figure 2d) and overlapped patterns indicative of bi- and trilayer graphene (Figure 2i,n), respectively.[31] In addition, the selected area electron diffraction (SAED) collected from respective surfaces displayed distinct hexagonal pattern without any halo (Figure. 2e,j,o) suggests a highly crystalline nature of the graphene.[20,28] A line passing through the $(1\bar{2}10)$–$(0\bar{1}10)$–$(\bar{1}010)$–$(\bar{2}110)$ axis also provides evidence of the layers of graphene.[20,28] While intense $(0\bar{1}10)$ and $(\bar{1}010)$ peaks compared to $(1\bar{2}10)$ and $(\bar{2}110)$ peaks indicate single layer, intense $(1\bar{2}10)$ and $(\bar{2}110)$ peaks compared to $(0\bar{1}10)$ and $(\bar{1}010)$ peaks indicate more than one layer.[20] More images of graphene flakes along with their FFT and SAED patterns are provided as Supporting Information images (Figures S11,12).

It is worth mentioning here that throughout the TEM observation, we rarely came across any flake with thickness more than a few layers. To back this claim, we carried out extensive thickness identification using atomic force microscopy. We measured over 450 flakes to identify the layer thickness of our exfoliated graphene. Figure 2p–s shows AFM

https://dx.doi.org/10.1021/acsnano.0c09451
ACS Nano 2021, 15, 1775–1784

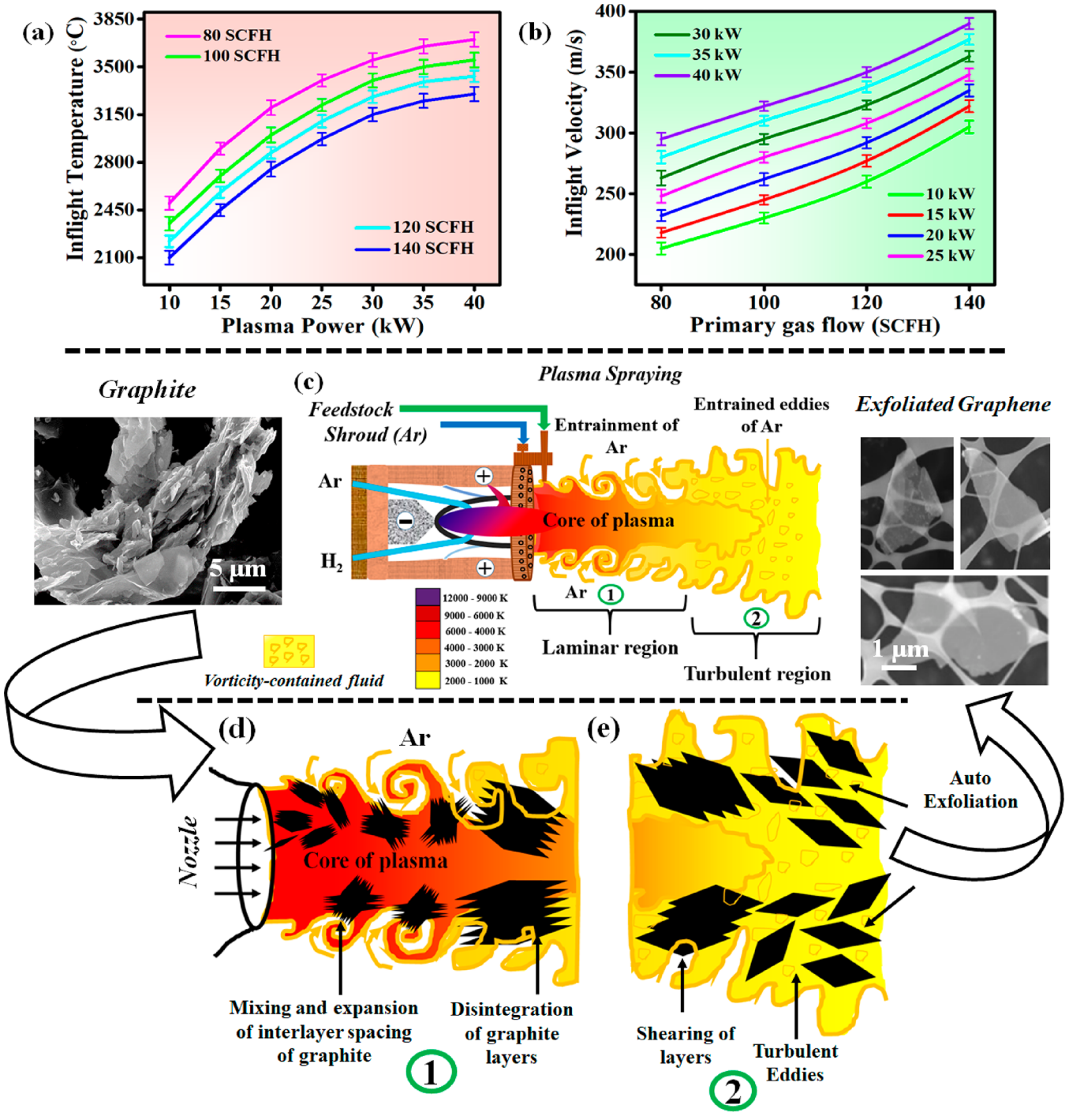

Figure 4. (a) Plot of plasma power vs in-flight temperature and (b) primary gas flow rate vs in-flight velocity showing linear trend for all sets of gas flow rate and plasma power. (c) Schematic representation of the exfoliation mechanism of graphite. (d) Magnified view of the laminar region of a plasma plume of part c. (e) Magnified verison of the turbulent region.

image of graphene (more images in Supporting Information S13) with their corresponding height profiles as well as flake thickness and size histogram. Similar to our TEM observations, almost all the measured flakes were less than 2 nm thick, with the majority of flakes below 1 nm thick providing unambiguous evidence of single layer to few layer graphene. Reports describe that the thickness of a single-layer graphene measured by AFM typically ranges between 0.6 and 1 nm.[28,32] A thickness histogram of over 400 arbitrary flakes presented higher selectivity toward single-layer graphene (85%), with 15% bi–trilayers (Figure 2r). Thus, we believe that in our samples, the graphite has been extensively exfoliated to single-layer to few-layer graphene (≤3 layers). The flake size histogram indicates the length of 1−3 μm (Figure 2s), also in agreement with the low magnification SEM image showing many flakes (Figure 2t).

The structural integrity of the exfoliated graphene was evaluated using Raman spectroscopy. We collected Raman spectra from what we believe are single-layer, bilayer, and trilayer graphene (Figure 3a). One key feature that

https://dx.doi.org/10.1021/acsnano.0c09451
ACS Nano 2021, 15, 1775−1784

distinguishes the number of layers in graphene is the shape, size, and intensity of 2D peak. As an example, a single-layer graphene displays a sharp and symmetric 2D peak, while multilayers with Bernal (AB) stacking shows complex 2D shape fitted by multiple Lorentzian lines.[33] The Raman spectrum of the monolayer graphene more closely resembles that of liquid exfoliated graphene rather than broad and highly disordered spectrum of thermally reduced rGO.[20,21] However, as the Raman beam spot size (<2 μm) is smaller than most of the exfoliated graphene, it is safe to assume that the D peak might be dominated by the edge effect. Yet, we cannot completely rule out any contribution from basal plane defects induced during the exfoliation process. We therefore performed Raman mapping and *in situ* AFM of the graphene flakes. Raman map of G and D band (Figure 3b,c) indicates higher defect density along the edges of the graphene. *In situ* Raman analysis of the same flake demonstrated no defect in the midportion of the flake, while an intense D band appears at the edge (Figure 3d,e). This suggests that D band measured here is associated with the flake edges. We note that the I_D/I_G ratio along the edge (~0.2) is similar to that of LPEG and significantly lower than that of ball milled graphene, indicating the defect-free nature of our exfoliated graphene.[21−23]

It is crucial to ascertain the quality of graphene after exfoliation. XPS was used to characterize the surface chemistry of our exfoliated graphene. The XPS results (Figure 3f) indicate that exfoliated graphene consists of in-plane oxygen concentration of ~4.5 at. %, which is lower than 6.1 at. % of noncovalently bonded adsorbed oxygen in graphite. The atomic ratio of carbon and oxygen (C/O) is ~21.2, which is higher than previously reported value of GO, rGO, and EcG and is close to LPEG and CVD grown graphene.[14,18,34] Increase in the C/O ratio is an indication of removal of some oxygen containing functional groups during plasma spraying. The high resolution of the C 1s peak of exfoliated graphene can be fitted into three peaks at 284.6, 287.1, and 290.9 eV. The first two correspond to the C—C and C═O bonds, respectively (Figure 3g).[17,28,35] The 290.9 eV peak related to the $\pi-\pi^*$ transition is clearly visible after exfoliation, indicating that the conjugated aromatic structure is preserved after exposure to very high temperature.[36] Additionally, FTIR revealed nearly featureless spectra for exfoliated graphene which is in contrast to the spectra of GO (Supporting Information S14).[37] This indicates that we produce graphene rather than some form of derivatized graphene. Figure 3h compares our exfoliated graphene with graphene obtained from various methods/sources. Comparison is made based on two important factors (carbon content, C and % of sp^2) which define the quality of graphene. We observe that with C = 95.5% and sp^2 % = 95% the quality of our exfoliated graphene is much higher than that of GO and rGO and are comparable with that of EcG, LEG, and CVD graphene.

We then try to explore the mechanism which could have aided the exfoliation of graphite to graphene. The entire exfoliation step can mainly be divided into three stages: thermal shock of graphite by hot plasma (stage-1), and two-stage shearing of the graphite particle in laminar (stage-2) as well as in turbulent region (stage-3) of the plasma plume. Since the thermal and kinetic history of the in-flight particle has an important role in thermal shock and subsequent shearing of graphite particle, the temperature and velocity of the sprayed graphite are scrutinized with respect to exfoliation efficiency.

Figure 4a,b illustrates the temperature and velocity of the graphite particle captured by the in-flight particle diagnostic sensor. With an increasing plasma power from 10 to 40 kW and primary gas flow rate from 80 to 140 SCFH, both temperature and velocity of graphite particle increases. Now, referring the schematic in Figure 4c and magnified view in Figure 4d, as soon as the graphite particles are injected into the laminar region of hot plasma, it experiences thermal shock at high temperature (3430 °C). Note that at such high temperature, any damage in graphite was prevented by the use of an inert argon gas shroud and the short residence time (in μs) of graphite particle in hot plasma due to the technique's high cooling rate 10^6 K/s.[35] In addition, the heat transfer to the graphite particle could have an important role in preventing the particle from damage. Assuming the boundary condition of the graphite powder to be symmetric, the heat transfer within the particle could be approximated by the conduction equation (eq 1).[38]

$$\frac{\partial H}{\partial t} = \frac{1}{r^2}\frac{\partial}{\partial r}\left(K_p r^2 \frac{\partial T}{\partial r}\right) \quad (1)$$

where r is the radial distance from the center of the particle. H is the enthalpy of the graphite particle, having a thermal conductivity of K_p, and T is the temperature at the given radius. Hence, for a graphite particle with similar dimension, heat transfer will be more at higher temperature, which will certainly avoid the localized heating and further prevent any damage of the graphite.

The thermal shock will lead to an increase in graphitic interlayer spacing. The graphitic interlayer spacing (d) follows a nonlinear dependency with temperature (t) up to 2600 °C has already been demonstrated, as per the equation.[39]

$$d = 3.357 + 91.9 \times 10^{-6} t + 5.3 \times 10^{-9} t^2 \quad (2)$$

Since van der Waals attraction force is inversely proportional to r^6 (r is the distance between the molecules),[40] increased interlayer spacing upon thermal shock will lower the van der Waals force and results to that of a weakened graphite particle.

In parallel to thermal shock, weakened graphite particles also experience a shear force (stage-2) due to the combination of viscosity and velocity of the plume simultaneously in the laminar region.[41] By increasing the primary gas flow rate to 120 SCFH, the plume velocity increases, and subsequently, the velocity of the graphite particle reaches 350 m/s. Conversely, the viscosity of the plasma gas exponentially increases at higher temperature, and it will decelerate the forward moving graphite particle (for details, refer to Supporting Information, S15). Hence, this opposing force could help in shearing the graphitic layer and aid the exfoliation of the expanded graphite layers.

The already weakened and partially sheared graphite particle transcends downstream toward the turbulent region (Figure 4c,e) where it encounters the large-scale eddies of cold ambient gas (*i.e.*, shroud argon gas). Since these entrained cold eddies will have the higher density compare to their high temperature counterparts, entrapped graphite particle will experience greater inertia.[41] Consequently, the graphite particle will try to travel along the axial direction at much lower velocity, while the hot plasma plume travels with very high velocity due to the higher primary gas flow rate (120 SCFH). This is exactly the competing phenomena where the already weakened and initially sheared graphite particle again encounters strong shear between the graphitic layers resulting the autoexfoliation of graphene sheet.

https://dx.doi.org/10.1021/acsnano.0c09451
ACS Nano 2021, 15, 1775−1784

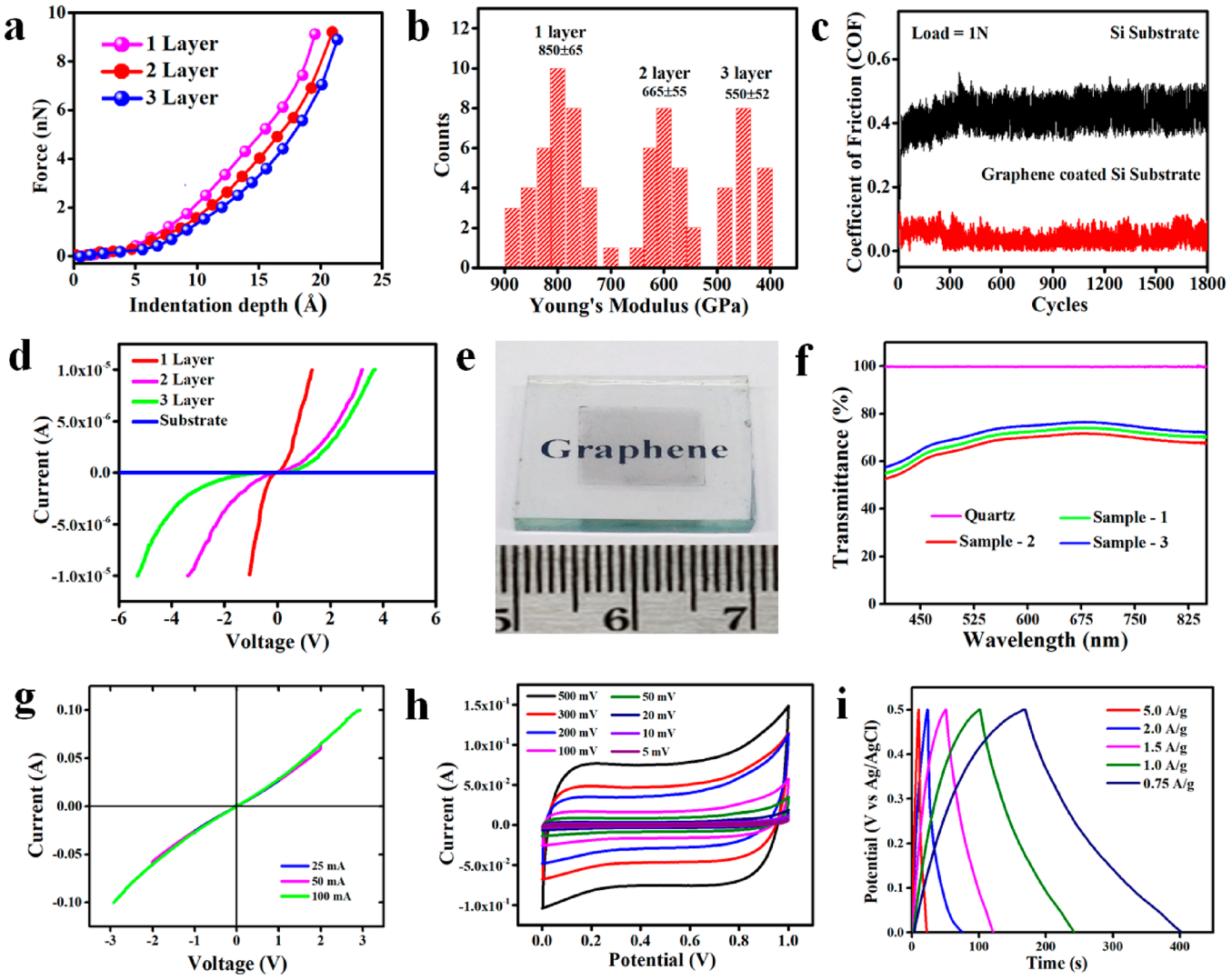

Figure 5. (a) AFM force−indentation depth curves of single-layer, bilayer, and trilayer graphene. (b) Histogram of Young's modulus for single-layer, bilayer, and trilayer graphene. (c) COF of graphene coated over Si wafer vs Si against a bare steel ball. (d) Current−voltage (*I*−*V*) curves for single-layer, bilayer, and trilayer graphene. (e) Digital image of graphene film over quartz. (f) Transmittance of film measured by UV−vis optical spectroscopy. Three samples tested yield transmittance of 69−72%. (g) *I*−*V* characteristics. Inset is the AFM to identify the thickness of the film. Suspension of exfoliated graphene in ethanol was spin coated over quartz to obtain the film. (h) Cyclic voltammetry curves of the graphene at different scan rates. (i) Galvanostatic charge−discharge curves at different current densities.

So, if the plasma gas velocity can further be increased by increasing the primary gas flow rate from 120 to 140 SCFH, ideally it should have efficient exfoliation having a greater number of single layers. However, it is to be noted that increasing the gas flow rate will cause the drop in in-flight particle temperature (3430 °C at P7G3, 3300 °C at P7G4) and the phenomena of thermal shock may be disturbed. To confirm our findings, we varied the process parameters from P7G3 (*T*: 3430 °C, *V*: 350 m/s) to P5G3 (*T*: 3280 °C, *V*: 323 m/s), and TEM analysis of the exfoliated graphene showed the presence of multilayer instead of 1−3 layers (Supporting Information S16). This has further verified our findings that the right combination of temperature and velocity will have an impact on the number of layers of graphene. With the more rigorous trials, the process sheets can further be designed to achieve the exact dependency of process parameters on the exfoliation of graphitic layers.

For commercial production of graphene, two of the most critical metrics are the yield and production rate. These metrics to some point have suffered from the lack of standardization. As an example, past studies simply divided the mass of exfoliated graphene by mass of original graphite to obtain yield without considering additional separation steps, which reduce yield.[17,42] Henceforth, studies overestimate yields up to 93% of the total parent mass under optimal conditions. Here, we define our yield as the product obtained after exfoliation and mild centrifugation. Note that our process does not require extensive cleaning of the collected supernatant such as solvent removal that reduces yield. Our laboratory-scale experiments result in yield up to 40% comparable with other exfoliation techniques (refer to Supporting Information S17 for more detailed information on yield). Additionally, we define our graphene production rate which is one of the most critical aspects to prototype industrialization. Our prototype lab-scale experiments demonstrated graphene production rate over 48 g/h. Additionally, it cost us around USD $1.12 to produce 1 g of graphene (Supporting Information S18). It is to be noted that production cost depends upon the local condition (*i.e.*,

https://dx.doi.org/10.1021/acsnano.0c09451
ACS Nano 2021, 15, 1775−1784

plasma gases, electricity charge, labor cost, *etc.*). Hence, this may be taken as reference. Although not comprehensive, we note that our production cost is lower than most of the commercially available single-layer or few-layer graphene.

A rigorous comparison was drawn against the literature available for gauging our exfoliated graphene in terms of a few essential factors including number of layers, quality of graphene, yield, and production rate of the protocol (Supporting Information S19). This indicates that no work portrays production rates above 48 g/h coupled with I_D/I_G intensity ratios below 0.20 (overall). In reality, 80% of the manuscripts visited had production rates below 1 g/h, far below that required for commercial production. Our C/O ratio and sp^2 are high enough to compete with high quality graphene.

Another important metric to realize in graphene commercialization is reproducibility. We produced graphene using the same optimized parameter (*P*: 40 kW, *G*: 120 SCFH) in a total of five (5) batches (Supporting Information S20). All batches were independently inspected for structural integrity and selectivity toward the number of layers. Raman spectra of all five batches demonstrated intense G and 2D bands at ∼1580 and 2719 cm^{-1}, respectively. A minor D band was also observed in all batches and is consistent with previous results. Thickness inspection using AFM shows that 75−85% of flakes are single layer.

The superlative properties of graphene make it ideal for all-encompassing applications both as standalone and as an additive. To date, more than 40 application areas have been identified where graphene has the potential to make a significant commercial impact.[1] Hence, in order to gauge the viability of our exfoliated graphene, we tested it in some applications that require high quality graphene in large quantities (details about the experiments have been discussed in Supporting Information S21). One major application area where graphene has already been utilized to its full spectrum is as strengthening additives, thanks to its exceptionally high Young's modulus (∼1 TPa).[43] We performed indentation using atomic force microscope to measure the Young's modulus of the exfoliated graphene (experimental details in Supporting Information S21a). The solid lines in Figure 5a shows the respective force−indentation depth curves of single, bi, and trilayer exfoliated graphene performed at constant incremental load of 10 nN. For each layer, a total of 40 loading/unloading curves were collected and the distribution of derived moduli were plotted as histograms (Figure 5b). The single-layer exfoliated graphene shows an effective Young's modulus of 850 ± 65 GPa, which reduces to 665 ± 55 and 550 ± 52 GPa for bi- and trilayer, respectively. Notably, the modulus of our exfoliated graphene is closer to the modulus of mechanically cleaved single layer graphene (1 TPa) measured using similar technique.[43] However, it is much higher than that of the GO (∼207 GPa), which is an indicator of defect-free graphene.[44] The bilayer and trilayer graphene show lower Young's modulus compared to that of the single-layer graphene. This is due to the weaker interlayer interaction in adjacent graphene layers which slide relative to each other upon indentation.[45] We performed macroscale lubricity test of the exfoliated graphene. Graphene deposited over Si wafer showed a very low coefficient of friction (COF = 0.03 ± 0.01) against the uncoated Si surface (0.42), while sliding with bare steel ball at 1 N loading (Figure 5c). Note that this ∼90% reduction in COF is encouraging, as a mere reduction of 20% friction can impact on cost in view of energy reserves and environmental benefits.[46] The COF remains consistent even for higher load (Supporting Information S21b). Layer-wise electrical conductivity of the graphene was confirmed using a conductive AFM (cAFM). The linear *I*−*V* curve (Figure 5d) for an individual single, bi, and trilayer graphene is representative of its excellent conductivity.[47] We also produced a thin film of the exfoliated graphene for potential transparent conductive coatings applications. Shown in Figure 5e is the digital image of the thin graphene film with thickness of ∼50 nm (Supporting Information S21d). The film is visually transparent with transmittance up to 73% at λ = 550 nm (Figure 5f). Note that this transmittance is little lower than commercially available ITO and FTO.[48,49] However, we believe that higher transmittance could be achieved by optimizing the thickness of the film and its post-processing. The film also has low sheet resistance of ∼30 Ω/sq (Figure 5g), which is much lower than films prepared using graphene obtained from other exfoliation techniques.[50] We performed electrochemical test to analyze its potential as energy storage devices like supercapacitors. The cyclic voltammetry (CV) curves of exfoliated graphene demonstrate near-perfect rectangular shape at different scan rate (Figure 5h), indicating pseudocapacitance behavior.[51] The curve follows the pseudocapacitive nature even at lower scan rate and is higher than that of graphite (Supporting Information S21e). The maximum specific capacitance obtained for exfoliated graphene is 375 F/g at 5 mV/s, comparable to 3D graphene architecture used for energy storage devices.[52,53] Furthermore, the galvanometric charge−discharge (GCD) curves at various current densities (Figure 5i) are highly symmetrical, indicating ideal capacitive behavior and excellent electrochemical reversibility. The specific capacitance obtained from GCD curves are comparable to that obtained by CV at scan rate 5 mV/s. Thus, we anticipate that this work will results in ultrafast production of the high quality and defect-free graphene powder in kilograms that can be used in diversified applications.

CONCLUSIONS

We demonstrated an ultrafast strategy to exfoliate graphite into high quality graphene with ∼85% selectivity of single layer without the use of any intercalants, chemicals, or solvent. This was achieved by the instantaneous temperature surge and two-stage shear at laminar and turbulent region of plume using a technology that is well established and highly scalable. Raman and XPS characterization ($I_D/I_G \approx 0$, C/O ≈ 21.2, sp^2 %: ∼95%) reveals high quality graphene with minimalistic defects. Laboratory tests demonstrated ultrahigh production capacity (48 g/h) indicating that scale-up of continuous graphene synthesis can be achieved without losing yield or quality. On top of that, the quality of graphene remained same for different batches demonstrating the reproducibility of the process. This straightforward method has the potential to provide sub-kilogram scale low-cost graphene (our laboratory-scale production cost: USD $1.12 per gram) that holds great promise for a large number of applications such as reinforcements, superlubric coatings, energy devices, and transparent conducting films. We believe that this work could be a game changer in the production of pristine graphene in large scale for numerous applications.

https://dx.doi.org/10.1021/acsnano.0c09451
ACS Nano 2021, 15, 1775−1784

EXPERIMENTAL METHODS

Exfoliation was performed using a plasma spray system (Oerlikon Metco, Switzerland) which uses a 9MB gun (Nozzle: GH 9MB733A). Refer to Supporting Information Movie S1 for the exfoliation process. Argon served as primary gas, while hydrogen was used as secondary gas for generating the plasma. All gases are 99.9% pure and were procured from Praxair Gasses Inc., India, unless otherwise mentioned. In a typical experiment, the graphite powder (procured from Sigma-Aldrich, Supporting Information S3) was fed into the powder feeder without any pretreatment. Argon was introduced inside the powder feeder and the chamber pressure was maintained at 20 Pa. The powder feeder was subjected to thorough vibration using an air vibrator (pressure: 10 Pa) for avoiding agglomeration of graphite powder. The argon (also used as carrier gas) carried the graphite powder through a coaxial cable (diameter: 1 mm) into the plasma gun. Powder feed rate was maintained at 120 g/h for all experiments. A custom-made inert atmosphere shroud which uses argon was fitted in the plasma gun to mimic inert atmosphere around the gun while in operation. An in-flight particle diagnostic sensor was positioned perpendicular 75 mm from the nozzle exit. More details about the main plasma spray system, shroud attachment, and in-flight particle diagnostic sensor is discussed in Supporting Information S2. The main plasma parameters varied throughout are the plasma power, P (10−40 kW) and primary gas flow G (80−140 SCFH), where the numbers in brackets correspond to the range of values used in this work (Supporting Information S4). A large number of experiments were performed at designated parameters (Supporting Information S5). After spraying, the resultant powders were centrifuged (1000 rpm, 1 h) to remove any unexfoliated graphite. The characterization methods used in this work and proof-of-concepts are all described in much greater detail in Supporting Information 21.

ASSOCIATED CONTENT

Supporting Information

The Supporting Information is available free of charge at https://pubs.acs.org/doi/10.1021/acsnano.0c09451.

Overview of graphene synthesis at high temperature, details of DC plasma system, optimization of spray parameters, characterizations of graphite and exfoliated graphene, cost and yield calculation, a table of comparison and detailed application setup (PDF)

Movie S1: Plasma spray exfoliation of graphite to graphene (MPG)

AUTHOR INFORMATION

Corresponding Author

Anup Kumar Keshri − *Plasma Spray Coating Laboratory, Metallurgical and Materials Engineering, Indian Institute of Technology Patna, Bihar 801106, India;* orcid.org/0000-0001-6929-5810; Phone: +91-612-3028184; Email: anup@iitp.ac.in

Authors

Aminul Islam − *Plasma Spray Coating Laboratory, Metallurgical and Materials Engineering, Indian Institute of Technology Patna, Bihar 801106, India*

Biswajyoti Mukherjee − *Plasma Spray Coating Laboratory, Metallurgical and Materials Engineering, Indian Institute of Technology Patna, Bihar 801106, India*

Krishna Kant Pandey − *Plasma Spray Coating Laboratory, Metallurgical and Materials Engineering, Indian Institute of Technology Patna, Bihar 801106, India*

Complete contact information is available at: https://pubs.acs.org/10.1021/acsnano.0c09451

Author Contributions

#A.I. and B.M. contributed equally to this work.

Notes

The authors declare no competing financial interest.

ACKNOWLEDGMENTS

Authors A. Islam, B. Mukherjee, K. K. Pandey, and A. K. Keshri, gratefully acknowledge the Indian Institute of Technology Patna for providing laboratory resources and financial support. A.I. also acknowledges SERB IMPRINT-II (IMP/2018/000620) for his fellowship assistance. Authors wish to thank O.S. Asiq Rahman for helpful discussions. The authors acknowledge SAIF, IIT Bombay for providing the HRTEM facility. Centre for Nanoscience, IIT Kanpur is also acknowledged for providing characterization facilities.

REFERENCES

(1) Barkan, T. Graphene: The Hype *versus* Commercial Reality. *Nat. Nanotechnol.* **2019**, *14*, 904−906.

(2) Kong, W.; Kum, H.; Bae, S.-H.; Shim, J.; Kim, H.; Kong, L.; Meng, Y.; Wang, K.; Kim, C.; Kim, J. Path towards Graphene Commercialization from Lab to Market. *Nat. Nanotechnol.* **2019**, *14*, 927−938.

(3) Kauling, A. P.; Seefeldt, A. T.; Pisoni, D. P.; Pradeep, R. C.; Bentini, R.; Oliverra, R. V. B.; Novoselov, S. K.; Neto, A. H. C. The Worldwide Graphene Flake Production. *Adv. Mater.* **2018**, *30*, 1803784.

(4) Wick, P.; Louw-Gaume, A. E.; Kucki, M.; Krug, H. F.; Kostarelos, K.; Fadeel, B.; Dawson, K. A.; Tretiach, M.; Benfenati, F.; Flahaut, E.; Gauthier, L.; Prato, M.; Bianco, A. Classification Framework for Graphene-Based Materials. *Angew. Chem., Int. Ed.* **2014**, *53*, 7714.

(5) Ye, R.; Tour, J. M. Graphene at Fifteen. *ACS Nano* **2019**, *13*, 10872−10878.

(6) Polsen, E. S.; McNerny, D. Q.; Viswanath, B.; Pattinson, S. W.; Hart, A. J. High-Speed Roll-to-Roll Manufacturing of Graphene Using a Concentric Tube CVD Reactor. *Sci. Rep.* **2015**, *5*, 10257.

(7) Bae, S.; Kim, H.; Lee, Y.; Xu, X.; Park, J.-S.; Zheng, Y.; Balakrishnan, J.; Lei, T.; Kim, R. H.; Song, Y. I.; Kim, Y.-J.; Kim, K. S.; Özyilmaz, B.; Ahn, J.-H.; Hong, B. H.; Iijima, S. Roll-to-Roll Production of 30-Inch Graphene Films for Transparent Electrodes. *Nat. Nanotechnol.* **2010**, *5*, 574−578.

(8) Li, X.; Cai, W.; An, J.; Kim, S.; Nah, J.; Yang, D.; Piner, R.; Velamakanni, A.; Jung, I.; Tutuc, E.; Banerjee, S. K.; Colombo, L.; Ruoff, R. S. Large-Area Synthesis of High-Quality and Uniform Graphene Films on Copper Foils. *Science* **2009**, *324*, 1312−1314.

(9) Muñoz, R.; Gómez-Aleixandre, C. Review of CVD Synthesis of Graphene. *Chem. Vap. Deposition* **2013**, *19*, 297−322.

(10) Voiry, D.; Yang, J.; Kupferberg, J.; Fullon, R.; Lee, C.; Jeong, H. Y.; Shin, S. H.; Chhowalla, M. High-Quality Graphene *via* Microwave Reduction of Solution-Exfoliated Graphene Oxide. *Science* **2016**, *353*, 1413−1416.

(11) Park, S.; Ruoff, R. S. Chemical Methods for the Production of Graphenes. *Nat. Nanotechnol.* **2009**, *4*, 217−224.

(12) Dreyer, D. R.; Park, S.; Bielawski, C. W.; Ruoff, R. S. The Chemistry of Graphene Oxide. *Chem. Soc. Rev.* **2010**, *39*, 228−240.

(13) Bagri, A.; Mattevi, C.; Acik, M.; Chabal, Y. J.; Chhowalla, M.; Shenoy, V. B. Structural Evolution during the Reduction of Chemically Derived Graphene Oxide. *Nat. Chem.* **2010**, *2*, 581−587.

(14) Stankovich, S.; Dikin, D. A.; Piner, R. D.; Kohlhaas, K. A.; Kleinhammes, A.; Jia, Y.; Wu, Y.; Nguyen, S. T.; Ruoff, R. S. Synthesis of Graphene-Based Nanosheets *via* Chemical Reduction of Exfoliated Graphite Oxide. *Carbon* **2007**, *45*, 1558−1565.

(15) Parvez, K.; Wu, Z. S.; Li, R.; Liu, X.; Graf, R.; Feng, X.; Müllen, K. Exfoliation of Graphite into Graphene in Aqueous Solutions of Inorganic Salts. *J. Am. Chem. Soc.* **2014**, *136*, 6083−6091.

(16) Yang, S.; Lohe, M. R.; Müllen, K.; Feng, X. New Generation Graphene from Electrochemical Approaches: Production and Applications. *Adv. Mater.* **2016**, *28*, 6213−6221.
(17) Yang, S.; Ricciardulli, A. G.; Liu, S.; Dong, R.; Lohe, M.; Becker, A.; Squillaci, M. A.; Samori, P.; Müllen, K.; Feng, X. Ultrafast Delamination of Graphite into High-Quality Graphene Using Alternating Currents. *Angew. Chem., Int. Ed.* **2017**, *56*, 6669−6675.
(18) Achee, T. C.; Sun, W.; Hope, J. T.; Quitzau, S. G.; Sweeney, C. B.; Shah, S. A.; Habib, T.; Green, M. J. High-Yield Scalable Graphene Nanosheet Production from Compressed Graphite Using Electrochemical Exfoliation. *Sci. Rep.* **2018**, *8*, 14525.
(19) Novoselov, K. S.; Geim, A. K.; Morozov, S. V.; Jiang, D.; Zhang, Y.; Dubonos, S. V.; Grigorieva, I. V.; Firsov, A. A. Electric Field Effect in Atomically Thin Carbon Films. *Science* **2004**, *306*, 666−669.
(20) Hernandez, Y.; Nicolosi, V.; Loyta, M.; Blighe, F. M.; Sun, Z.; De, S.; McGovern, I. T.; Holland, B.; Byrne, M.; Gun'Ko, Y. K.; Boland, J. J.; Niraj, P.; Duesberg, G.; Krishnamurthy, S.; Goodhue, R.; Hutchison, J.; Scardaci, V.; Ferrari, A. C.; Coleman, J. High-Yield Production of Graphene by Liquid-Phase Exfoliation of Graphite. *Nat. Nanotechnol.* **2008**, *3*, 563−568.
(21) Paton, K. R.; Varrla, E.; Backes, C.; Smith, R. J.; Khan, U.; O'Neill, A.; Boland, C.; Loyta, M.; Istrate, O. M.; King, P.; Higgins, T.; Barwich, S.; May, P.; Puczkarski, P.; Ahmed, I.; Moebius, M.; Pettersson, H.; Long, E.; Coelho, J.; O'Brien, S. E.; et al. Scalable Production of Large Quantities of Defect-Free Few-Layer Graphene by Shear Exfoliation in Liquids. *Nat. Mater.* **2014**, *13*, 624−630.
(22) Ciesielski, A.; Samorì, P. Graphene *via* Sonication Assisted Liquid-Phase Exfoliation. *Chem. Soc. Rev.* **2014**, *43*, 381−398.
(23) Buzaglo, M.; Bar, I. P.; Varenik, M.; Shunak, L.; Pevzner, S.; Regev, O. Graphite to Graphene: Total Conversion. *Adv. Mater.* **2017**, *29*, 1603528.
(24) Parviz, D.; Irin, F.; Shah, S. A.; Das, S.; Sweener, C. B.; Green, M. J. Challenges in Liquid Phase Exfoliation, Processing, and Assembly of Pristine Graphene. *Adv. Mater.* **2016**, *28*, 8796−8818.
(25) Luong, D. X.; Bets, K. V.; Algozeeb, W. A.; Stanford, M. G.; Kittrell, C.; Chen, W.; Salvatierra, R. V.; Ren, M.; McHugh, E. A.; Advincula, P. A.; Wang, Z.; Bhatt, M.; Guo, H.; Mancevski, V.; Shahsavaro, R.; Yakobson, B.; Tour, J. M. Gram-Scale Bottom-Up Flash Graphene Synthesis. *Nature* **2020**, *577*, 647−651.
(26) Lee, J. H.; Shin, D. W.; Makotchenko, V. G.; Nazarov, A. S.; Fedorov, V. E.; Kim, Y. H.; Choi, J. Y.; Kim, J. M.; Yoo, J. B. One-Step Exfoliation Synthesis of Easily Soluble Graphite and Transparent Conducting Graphene Sheets. *Adv. Mater.* **2009**, *21*, 4383−4387.
(27) Dato, A. Graphene Synthesized in Atmospheric Plasmas-A Review. *J. Mater. Res.* **2019**, *34*, 214−230.
(28) Matsumoto, M.; Saito, Y.; Park, C.; Fukushima, T.; Aida, T. Ultrahigh-Throughput Exfoliation of Graphite into Pristine 'Single-Layer' Graphene Using Microwaves and Molecularly Engineered Ionic Liquids. *Nat. Chem.* **2015**, *7*, 730−736.
(29) Ferrari, A. C.; Meyer, J. C.; Scardaci, V.; Casiraghi, C.; Lazzeri, M.; Mauri, F.; Piscanec, S.; Jiang, D.; Novoselov, K. S.; Roth, S.; Geim, A. K. Raman Spectrum of Graphene and Graphene Layers. *Phys. Rev. Lett.* **2006**, *97*, 187401.
(30) Cai, M.; Thorpe, D.; Adamson, D. H.; Schniepp, H. C. Methods of Graphite Exfoliation. *J. Mater. Chem.* **2012**, *22*, 24992−25002.
(31) Robertson, A. W.; Warner, J. H. Atomic Resolution Imaging of Graphene by Transmission Electron Microscopy. *Nanoscale* **2013**, *5*, 4079−4093.
(32) Zhang, J.; Yang, H.; Shen, G.; Cheng, P.; Zhang, J.; Guo, S. Reduction of Graphene Oxide *via* L-Ascorbic Acid. *Chem. Commun.* **2010**, *46*, 1112−1114.
(33) Bepete, G.; Anglaret, E.; Ortolani, L.; Morandi, V.; Huang, K.; Pénicaud, A.; Drummond, C. Surfactant-Free Single-Layer Graphene in Water. *Nat. Chem.* **2017**, *9*, 347−352.
(34) Yi, M.; Shen, Z.; Zhang, X.; Ma, S. Achieving Concentrated Graphene Dispersions in Water/Acetone Mixtures by the Strategy of Tailoring Hansen Solubility Parameters. *J. Phys. D: Appl. Phys.* **2013**, *46*, 025301.
(35) Mukherjee, B.; Rahman, O. S. A.; Islam, A.; Pandey, K. K.; Keshri, A. K. Deposition of Multiscale Thickness Graphene Coating by Harnessing Extreme Heat and Rapid Quenching: Toward Commercialization. *ACS Appl. Mater. Interfaces* **2019**, *11*, 25500−25507.
(36) Ganguly, A.; Sharma, S.; Papakonstantinou, P.; Hamilton, J. Probing the Thermal Deoxygenation of Graphene Oxide Using High-Resolution *in Situ* X-Ray-Based Spectroscopies. *J. Phys. Chem. C* **2011**, *115*, 17009−17019.
(37) Li, D.; Muller, M. B.; Gilje, S.; Kaner, R. B.; Wallace, G. C. Processable Aqueous Dispersions of Graphene Nanosheets. *Nat. Nanotechnol.* **2008**, *3*, 101−105.
(38) Westhoff, R.; Trapaga, G.; Szekely, J. Plasma-Particle Interactions in Plasma Spraying Systems. *Metall. Trans. B* **1992**, *23*, 683−693.
(39) Steward, E. G.; Cook, B. P.; Kellett, E. A. Dependence on Temperature of the Interlayer Spacing in Carbons of Different Graphitic Perfection. *Nature* **1960**, *187*, 1015−1016.
(40) Du, W.; Jiang, X.; Zhu, L. From Graphite to Graphene: Direct Liquid-Phase Exfoliation of Graphite to Produce Single- and Few-Layered Pristine Graphene. *J. Mater. Chem. A* **2013**, *1*, 10592−10606.
(41) Krejci, L.; Dolinek, I. V.; Ruzicka, B.; Chalupova, V.; Russ, S. Identification of the Laminar-Turbulent Transition Process in a Plasma Plume. *Plasma Chem. Plasma Process.* **1993**, *13*, 601−612.
(42) Abdelkader, A. M.; Cooper, A. J.; Dryfe, R. A. W.; Kinloch, I. A. How to Get Between the Sheets: A Review of Recent Works on the Electrochemical Exfoliation of Graphene Materials from Bulk Graphite. *Nanoscale* **2015**, *7*, 6944−6956.
(43) Lee, C.; Wei, X.; Kysar, J. W.; Hone, J. Measurement of the Elastic Properties and Intrinsic Strength of Monolayer Graphene. *Science* **2008**, *321*, 385−388.
(44) Suk, J. W.; Piner, R. D.; An, J.; Rouff, R. S. Mechanical Properties of Monolayer Graphene Oxide. *ACS Nano* **2010**, *4*, 6557−6564.
(45) Lipatov, A.; Lu, H.; Alhabeb, M.; Anasori, B.; Gruverman, A.; Gogotsi, Y.; Sinitskii, A. Elastic properties of 2D $Ti_3C_2T_x$ MXene Monolayers and Bilayers. *Sci. Adv.* **2018**, *4*, eaat0491.
(46) Berman, D.; Deshmukh, S. A.; Sankaranarayan, K. S. R. S.; Erdemir, A.; Sumant, A. V. Macroscale Superlubricity Enabled by Graphene Nanoscroll Formation. *Science* **2015**, *348*, 1118−1122.
(47) Martin-Olmos, C.; Rasool, H. I.; Weiller, B. H.; Gimzewski, J. K. Graphene MEMS: AFM Probe Performance Improvement. *ACS Nano* **2013**, *7*, 4164−4170.
(48) Wang, S. J.; Geng, Y.; Zheng, Q.; Kim, J. K. Fabrication of Highly Conducting and Transparent Graphene Films. *Carbon* **2010**, *48*, 1815−1823.
(49) Wang, X.; Zhi, L.; Müllen, K. Transparent, Conductive Graphene Electrodes for Dye-Sensitized Solar Cells. *Nano Lett.* **2008**, *8*, 323−327.
(50) Ma, Y.; Zhi, L. Graphene-Based Transparent Conductive Films: Material Systems, Preparation and Applications. *Small Methods* **2019**, *3*, 1800199.
(51) Li, L.; Zhang, J.; Peng, Z.; Li, Y.; Gao, C.; Ji, Y.; Ye, R.; Kim, N. D.; Zhong, Q.; Yang, Y.; Fei, H.; Ruan, G.; Tour, J. M. High-Performance Pseudo-Capacitive Micro-Supercapacitors from Laser-Induced Graphene. *Adv. Mater.* **2016**, *28*, 838−845.
(52) Liu, J.; Zhang, J.; Peng, Z.; Li, Y.; Gao, C.; Ji, Y.; Ye, R.; Kim, N. D.; Zhong, Q.; Yang, Y.; Fei, H.; Ruan, G.; Tour, J. M. Charging Graphene for Energy. *Nat. Nanotechnol.* **2014**, *9*, 739−741.
(53) Cao, X.; Shi, Y.; Shi, W.; Lu, G.; Huang, X.; Yan, Q.; Zhang, Q.; Zhang, H. Preparation of Novel 3D Graphene Networks for Supercapacitor Applications. *Small* **2011**, *7*, 3163−3168.

https://dx.doi.org/10.1021/acsnano.0c09451
ACS Nano 2021, 15, 1775−1784